

Proxy dependence of the temporal pattern of deglacial warming in the tropical South China Sea: toward resolving seasonality

Stephan Steinke^{a,*}, Markus Kienast^b, Jeroen Groeneveld^a, Li-Chuan Lin^c, Min-Te Chen^c,
Rebecca Rendle-Bühning^a

^aDFG-Forschungszentrum "Ozeanränder"-Research Center Ocean Margins (RCOM), Universität Bremen, Postfach 33 04 40, D-28334, Bremen, Germany

^bDepartment of Oceanography, Dalhousie University, Halifax, Nova Scotia, Canada

^cInstitute of Applied Geosciences, National Taiwan Ocean University, Keelung, Taiwan

Received 6 July 2007; received in revised form 29 November 2007; accepted 12 December 2007

Abstract

Sea surface temperatures (SSTs), reconstructed from two *Globigerinoides ruber* (white) morphotypes (*G. ruber* sensu stricto, (s.s.); *G. ruber* sensu lato, (s.l.)) Mg/Ca and alkenones (U_{37}^K) from core MD01-2390 from the tropical South China Sea (SCS) during the last deglaciation reveal a proxy-dependent discrepancy in the temporal pattern of the deglacial warming. Alkenone data suggest that the deglacial warming is punctuated by a decrease in temperature between ~17 and 15 ka BP, corroborating previously published alkenone U_{37}^K SST records from the southern SCS. Within dating uncertainties, this cooling is coeval with the Heinrich Event 1 (H1) time interval in the North Atlantic region, underscoring the imprints of northern hemisphere forcing on tropical SCS ocean temperatures. The deglacial U_{37}^K SST minimum is also paralleled by a maximum in *G. ruber* morphotype-specific $\delta^{18}O$. *G. ruber* Mg/Ca SST estimates suggest a morphotype-specific record of SSTs during the time interval of H1. Whereas *G. ruber* s.s. imply a continuous warming starting around 18 ka BP without any marked response to H1, *G. ruber* s.l.-based Mg/Ca SST estimates reveal a cooling around ~17–15 ka BP similar to the H1 interval cooling seen in the alkenone SST record. Similar proxy-dependent differences in deglacial surface water warming have been recorded in the eastern equatorial Pacific, implying a common pattern on both sides of the tropical Pacific Ocean. We submit that this discrepancy could be due to differences in seasonality of planktonic foraminifera *G. ruber* morphotypes and alkenone-producing algae.

© 2007 Elsevier Ltd. All rights reserved.

1. Introduction

Determining the timing and magnitude of tropical Pacific SST variability is a critical problem in palaeoclimatology, because the thermal history of the tropical Pacific is thought to play a vital role in modulating global climate on seasonal, interannual (El Niño-Southern Oscillation (ENSO)), millennial, and orbital time scales (Cane, 1998; Clement et al., 1999). Moreover, atmospheric modelling studies suggest that tropical SST variations could have been a potential trigger of northern hemisphere deglaciation (Rodgers et al., 2003; Hostetler et al., 2006).

The importance of regional tropical SST patterns in modulating Last Glacial Maximum (LGM) climate has been further highlighted by atmospheric circulation modelling studies (e.g. Yin and Battisti, 2001). Thus, an accurate assessment of the temporal pattern and magnitude of tropical SST changes is of crucial importance for a mechanistic understanding of the oceanographic and climatic changes that occurred during the last deglaciation.

Past SSTs are estimated using a variety of different proxies, including planktonic foraminiferal transfer functions, the alkenone unsaturation index and Mg/Ca ratios in planktonic foraminiferal shells (e.g. Wefer et al., 1999; Lea, 2003). However, significant disagreements in the amplitude and/or timing of SST changes have been observed when a multi-proxy approach for reconstructing past SSTs has been applied on the same sample material (e.g. Nürnberg

*Corresponding author. Tel.: +49 421 218 65882;
fax: +49 421 218 65515.

E-mail address: ssteinke@uni-bremen.de (S. Steinke).

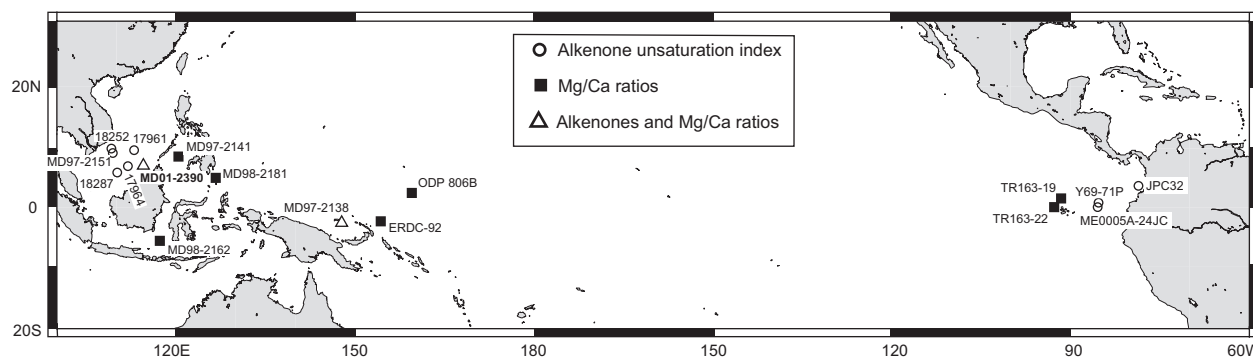


Fig. 1. Map of the equatorial Pacific showing the location of core MD01-2390. The locations of other cores discussed in the text are also indicated: 18287 and 18252 (Kienast et al., 2001), MD97-2151 (Zhao et al., 2006), 17964 and 17961 (Pelejero et al., 1999a), MD97-2141 (Rosenthal et al., 2003), MD98-2181 (Stott et al., 2002), MD98-2162 (Visser et al., 2003), MD97-2138 (de Garidel-Thoron, 2007), ERDC-92 (Palmer and Pearson, 2003), ODP 806B (Lea et al., 2000), TR163-19 (Lea et al., 2000), TR163-22 (Lea et al., 2006), ME0005A-24JC (Kienast et al., 2006), Y69-71P (Prahel et al., 2006) and JPC32 (Pahnke et al., 2007). Different plot symbols indicate sites with SST estimates either derived from planktonic foraminiferal Mg/Ca ratios (squares), alkenones (dots) or multiple proxies (Mg/Ca and alkenones; triangles).

et al., 2000 for the equatorial Atlantic; Steinke et al., 2001 and Chen et al., 2005 for the South China Sea; Cayre and Bard, 1999 for the Indian Ocean; de Garidel-Thoron et al., 2007 for the western equatorial Pacific).

In a recent review, Mix (2006) highlighted the contrasting patterns of deglacial warming as recorded by planktonic foraminiferal Mg/Ca ratios and the alkenone unsaturation index in the eastern equatorial Pacific (EEP). Whereas Mg/Ca data suggest a gradual, continuous warming of the EEP starting at ~19 ka BP (cores TR163-19 and TR163-22, Lea et al., 2006; see Fig. 1 for core locations), alkenone unsaturation data (core Y69-71P, Fig. 1; Prahel et al., 2006) in the same region reveal a decrease in temperature during the early deglaciation (20–15 ka BP), exactly at the time Mg/Ca ratios suggest a warming. A similar early deglacial cold event has also been observed in two high-resolution alkenone-based SST records from two other sites in the EEP and has been interpreted to reflect a regional cooling in response to H1 (core ME0005A-24JC, Kienast et al., 2006; core JPC32, Pahnke et al., 2007, Fig. 1). In the western equatorial Pacific, Mg/Ca records again suggest a continuous warming trend starting at ± 19 ka BP (Sulu Sea, core MD97-2141, Rosenthal et al., 2003; Makassar Strait, MD98-2162, Visser et al., 2003, and the Western Pacific Warm Pool, core MD97-2138 de Garidel-Thoron et al., 2007; ODP 806B, Lea et al., 2000; MD98-2181, Stott et al., 2002; Fig. 1). This implies a common trend for deglacial warming as recorded by planktonic foraminiferal Mg/Ca in the “open” equatorial Pacific. Again contrary to the Mg/Ca records, alkenone-derived SST records from the marginal, southern SCS suggest a cooling around 17–15 ka BP (see the recent compilation of Kiefer and Kienast, 2005). Inspired by Mix’ commentary, we present new SST estimates based on the alkenone unsaturation index and on morphotype-specific *G. ruber* Mg/Ca ratios from a single core (MD01-2390) located in the southern SCS, in an attempt to shed more light on the discrepancy between SST

estimates recorded by the two proxy carriers. Our study is focused on the last deglaciation, a time period for which previously published records indicate the largest discrepancy between both proxies.

2. Material and methods

CALYPSO gravity core MD01-2390 (06°38.12 N; 113°24.56 E; water depth of 1545 m) was collected during R/V *Marion Dufresne* cruise 122/IMAGES VII—WEPA-MA (Leg 1) on the Nansha Shallow of the southern SCS (Fig. 1). The age model of core MD01-2390 is based on AMS-¹⁴C dating and is corroborated by a planktonic foraminiferal *G. ruber* s.s. $\delta^{18}\text{O}$ record that was further visually compared to previously published ¹⁴C-dated oxygen isotope records of the southern SCS (Pelejero et al., 1999a; Wang et al., 1999; Kienast et al., 2001; Steinke et al., 2001; Chen et al., 2005). The age model and the planktonic foraminiferal *G. ruber* s.s. $\delta^{18}\text{O}$ record have been published and discussed previously by Steinke et al. (2006). Sedimentation rates range from ~70 cm/ka during the glacial interval to 30 cm/ka during the Holocene (Steinke et al., 2006), in agreement with neighbouring cores from the southern SCS (e.g. 18287 and 18252, Kienast et al., 2001; 17964, Wang et al., 1999).

Alkenone determinations for the depth interval 300–750 cm (10–19 ka BP; at 10-cm intervals, equivalent to ~150-yr sample spacing) were carried out on freeze-dried and homogenized sediments (~1.5 g). Alkenones were extracted by ultrasonication using a sequence of two solvents: dichloromethane and methanol. An aliquot of the lipid extract was separated into four fractions [F1: 3 ml of hexane; F2: 3 ml of hexane:toluene (3:1); F3: 4 ml of toluene; F4: 3 ml of toluene:methanol (3:1)] by silica gel column chromatography (SiO₂ with 5% distilled water; i.d., 5.5 mm; length, 45 mm). *n*-C₂₄D₅₀ and *n*-C₃₆H₇₄ were added as internal standards into the F1 (*n*-alkenes) and F3 (alkenones and alkenoates) fractions, respectively. Gas

chromatography was conducted using a Hewlett Packard 5890 series N gas chromatograph (GC) with cool on-column injection and electron pressure control systems and a flame ionization detector (FID) at the National Taiwan Ocean University, Keelung. Samples were dissolved in hexane. Helium was used as a carrier gas, and the flow velocity was maintained at 30 cm/s. For the analyses of the F3 (alkenones and alkenoates) fraction, the oven temperature was programmed from 70 to 290 °C at 20 °C/min, 290 to 310 °C at 0.5 °C/min, and then isothermal at 310 °C for more than 30 min. The alkenones were identified by their gas chromatographic retention times by analogy with a synthetic standard (provided by M. Yamamoto, Hokkaido University, Japan). Peak areas were converted to the alkenone unsaturation index ($U_{37}^{K'}$), and SSTs were calculated using the equation developed by Pelejero and Grimalt (1997), which was established by correlating the $U_{37}^{K'}$ index in core-top sediments from the SCS with annually averaged water column temperatures for the top 30 m. The mean standard error of estimated temperatures for various temperature equations is around 1 °C (e.g. Conte et al., 2006).

In this study, we developed continuous LGM-Holocene morphotype-specific stable oxygen isotope and Mg/Ca records by analyzing *G. ruber* s.s. and *G. ruber* s.l. following the definition of Wang (2000). The main reason for performing morphotype-specific analyses is that a comparison of stable oxygen isotopes and Mg/Ca analyses of the two *G. ruber* morphotypes (*G. ruber* s.s. and *G. ruber* s.l.) from core-top and downcore samples showed statistically significant differences in stable oxygen isotopes (Wang, 2000; Löwemark et al., 2005; Steinke et al., 2005) and Mg/Ca ratios (Steinke et al., 2005; see discussion below).

Core MD01-2390 was sampled at 5-cm intervals (12.5–502.5 cm) and 10-cm intervals (512.5–992.5 cm) for oxygen isotope analyses on *G. ruber* s.s. and at regular 10-cm intervals for analyses on *G. ruber* s.l. Oxygen isotope ratios were determined on samples composed of 15–20 specimens from the 250 to 350 µm size fraction. Isotopic analyses of *G. ruber* s.s. and *G. ruber* s.l. samples were performed using a Finnigan MAT 251 mass spectrometer with an automated carbonate preparation device at the Leibniz Laboratory (University of Kiel) and at the Department of Geosciences (University of Bremen), respectively. The external standard errors of the stable oxygen and carbon isotope analyses at the Kiel and Bremen MAT 251 are <0.08‰ and <0.06‰, respectively.

Mg/Ca analyses on *G. ruber* s.s. and *G. ruber* s.l. were run on a subset of samples with 5–40 cm spacing (~150–300 yr sample). For each sample, approximately 30–40 specimens (~330–420 µg) of both *G. ruber* (white) morphotypes were picked out of the 250–350 µm fraction. Foraminiferal tests were cleaned in successive steps following the cleaning protocol developed by Barker et al. (2003) and analysed on a Perkin-Elmer Optima 3300R ICP-OES at the Department of Geosciences, University of Bremen. Standards and replicate analyses gave a mean

reproducibility of ± 0.11 mmol/mol in Mg/Ca. *G. ruber* s.s. samples of the depth interval 12.5–422.5 cm (1–14 ka BP) were analysed on a Q-ICPMS (Agilent 7500s), housed at the Department of Geosciences, National Taiwan University (see Steinke et al., 2006 for details). The precision and external uncertainty are 0.1–0.2% and 0.4%, respectively (Shen et al., 2007). The comparability of the Mg/Ca values of the two laboratories has been tested by replicate analyses of late Holocene samples. The mean average difference of both laboratory measurements is ± 0.15 mmol/mol in Mg/Ca.

Mn/Ca, Fe/Ca and Al/Ca were determined in conjunction with Mg/Ca because clay contamination (e.g. Barker et al., 2003) and the occurrence of syn-sedimentary and post-depositional Mn-oxide precipitates and Mn-rich carbonate coatings (e.g. Pena et al., 2005; Weldeab et al., 2006) can exert a significant control on the Mg/Ca ratios, resulting in elevated Mg/Ca ratios and thus by inference in overestimated SSTs. Our results indicate no significant Mg contributions by Mn-oxides or Mn-rich carbonates or clays. Post-depositional, partial dissolution can exert an important control on Mg/Ca ratios (e.g. Brown and Elderfield, 1996; Rosenthal et al., 2000; Regenberget al., 2006). However, carbonate preservation is excellent in this core. The core is located above the modern-day calcite lysocline, which is approximately at 3000 m water depth (Rottman, 1979; Miao et al., 1994). Excellent carbonate preservation is further attested by the occurrence of pteropods throughout the core (Steinke et al., 2006). We believe that variations in foraminiferal Mg/Ca over the last 25 ka are therefore primarily driven by temperature rather than preferential removal of Mg ions during calcite dissolution. Assuming that Mg/Ca ratios of both *G. ruber* morphotypes have the same temperature dependence, Mg/Ca ratios were converted to SST by means of the species-specific calibration for *G. ruber* (white; size fraction 250–350 µm; Dekens et al., 2002): $\text{Mg/Ca (mmol/mol)} = 0.38 \exp[0.09 \text{ SST (}^\circ\text{C)}]$. The standard error of estimates for various temperature equations derived from core-top and trap calibrations is typically in the range of 0.5–1.0 °C (Elderfield and Ganssen, 2000; Lea et al., 2000; Dekens et al., 2002; Anand et al., 2003).

3. Results and discussion

3.1. Temporal patterns of deglacial SST changes in the southern SCS

SST estimates based on alkenones ($U_{37}^{K'}$) and morphotype-specific *G. ruber* (white) Mg/Ca of core MD01-2390 display significant differences during the last deglaciation (Fig. 2). There are several important aspects of this discrepancy. The alkenone data reveal a distinct cooling between 17 and 15 ka BP (Figs. 3 and 4) that is \pm coeval with the North Atlantic Heinrich Event 1 (H1). This period of cooling is in agreement with previously published alkenone records from this region (Pelejero et al., 1999a;

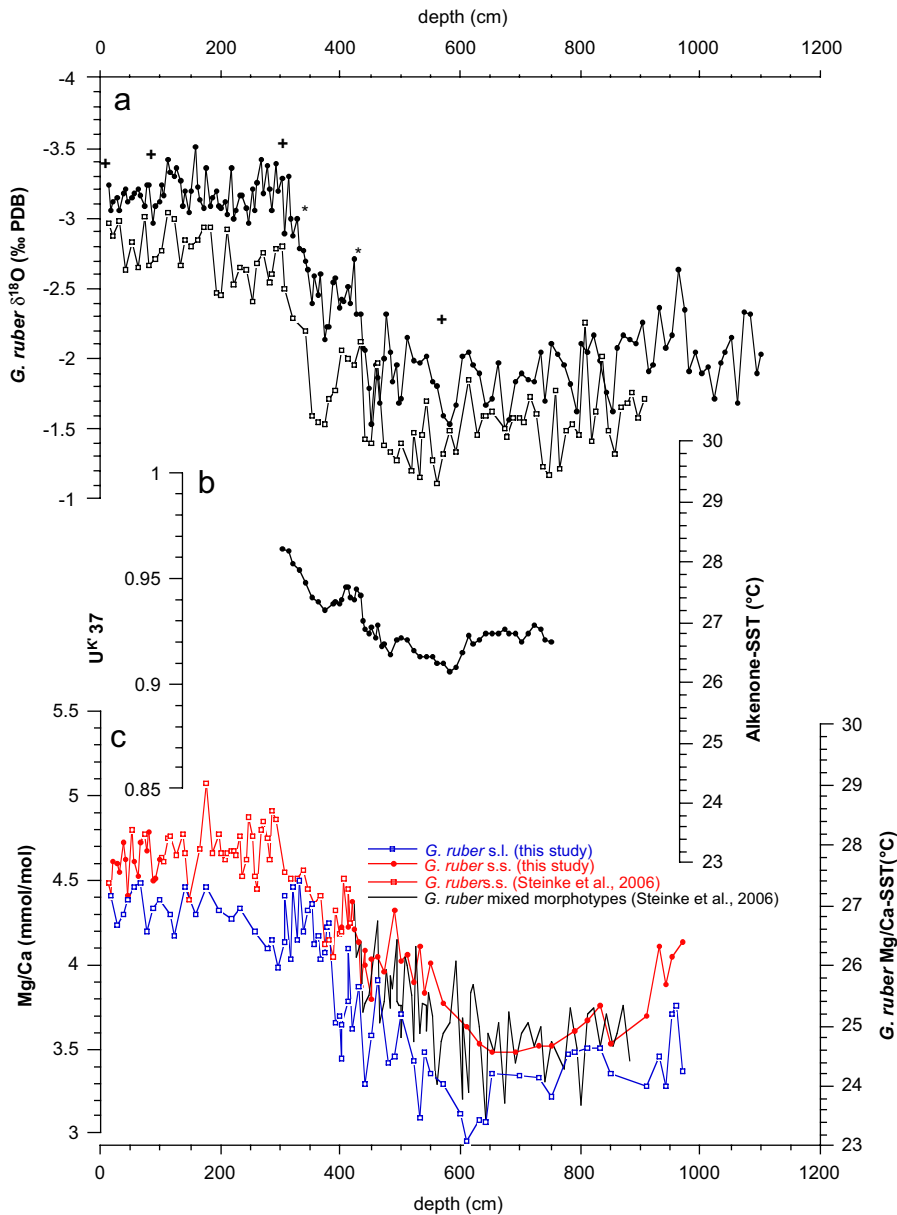


Fig. 2. (a) Oxygen isotope records of *G. ruber sensu stricto* (s.s.; solid dots) and *G. ruber sensu lato* (s.l.; open squares), (b) U_{37}^K index and alkenone SST estimates, and (c) Mg/Ca (red: *G. ruber* s.s., Steinke et al., 2006, this study; blue: *G. ruber* s.l., this study; black: mixed morphotypes, Steinke et al., 2006) and SST estimates from core MD01-2390, plotted vs depth in core (cm). Crosses and asterisks above the oxygen isotope records mark AMS- ^{14}C dates and analog ages (based on $\delta^{18}O$) used for the age model, respectively. Details of the age model are given in Steinke et al. (2006).

Zhao et al., 2006). The absolute U_{37}^K -SST estimates in core MD01-2390 in comparison with other cores from this region, however, are constantly positively offset by 1–1.5 °C for the time interval sampled (Fig. 3). This offset is most likely reflective of a NW–SE surface water temperature gradient, analogous to the present-day increase in SSTs from the NW to the SE southern SCS (Fig. 3). Despite this offset in absolute SST estimates, all southern SCS U_{37}^K -SST records are in good agreement in recording the major features during the glacial-interglacial transition, i.e., in particular the cooling during the time interval of H1, a rapid increase in temperature (~ 1 °C) around 15 ka BP and a subtle cooling or temperature

plateau during the Younger Dryas (YD). It has been suggested that the rapid SST increase at 15 ka BP is synchronous with the Bølling-warming observed in Greenland ice cores (Kienast et al., 2001; Steinke et al., 2001), most likely representing a strong atmospheric link to the climate history of the North Atlantic realm (Kiefer and Kienast, 2005).

Unlike in the previously published Mg/Ca record by Steinke et al. (2006), the use of morphotype-specific samples instead of samples composed of a mixture of different morphotypes significantly minimized the noise of the Mg/Ca records (Figs. 2 and 4). The Mg/Ca analyses of the two *G. ruber* morphotypes (*G. ruber* s.s. and *G. ruber*

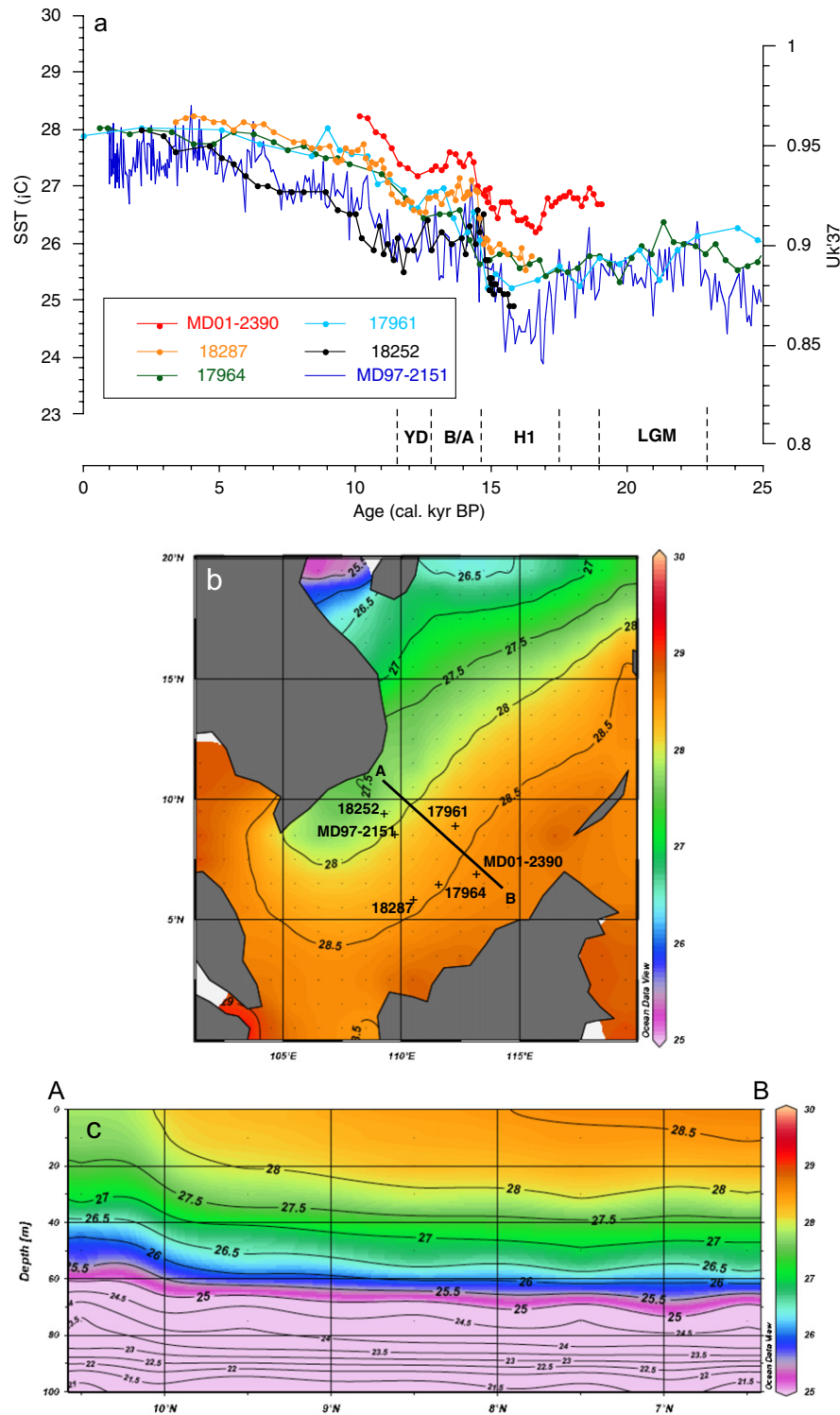


Fig. 3. Comparison of alkenone SST records from the southern South China Sea (SCS). (a) $U_{37}^{K'}$ index and alkenone SST data from southern SCS cores (18287 and 18252, Kienast et al., 2001; MD97-2151, Zhao et al., 2006; 17964 and 17961, Pelejero et al., 1999a; MD01-2390, this study). All SST estimates are calculated using the equation $UK'_{37} = 0.031T + 0.092$, which was established by correlating the $U_{37}^{K'}$ index in SCS core-top sediments with annually averaged water column SSTs for the top 30 m, Pelejero and Grimalt, 1997). YD = Younger Dryas; B/A = Bølling-Allerød; H1 = Heinrich event 1; LGM = Last Glacial Maximum); (b) Modern annual sea surface temperatures (in °C) at 0 m water depth (Ocean Data View; Schlitzer, 2007) and locations of cores shown in panel (a); (c) Temperature distribution along section A–B. See figure (b) for the position of section A–B (Ocean Data View; Schlitzer, 2007). Note the good agreement between the modern-day NW-SE SST gradient in the SCS and the increase in absolute $U_{37}^{K'}$ SST estimates from sites 18253 and MD97-2151 in the NW to site MD01-2390 in the SE.

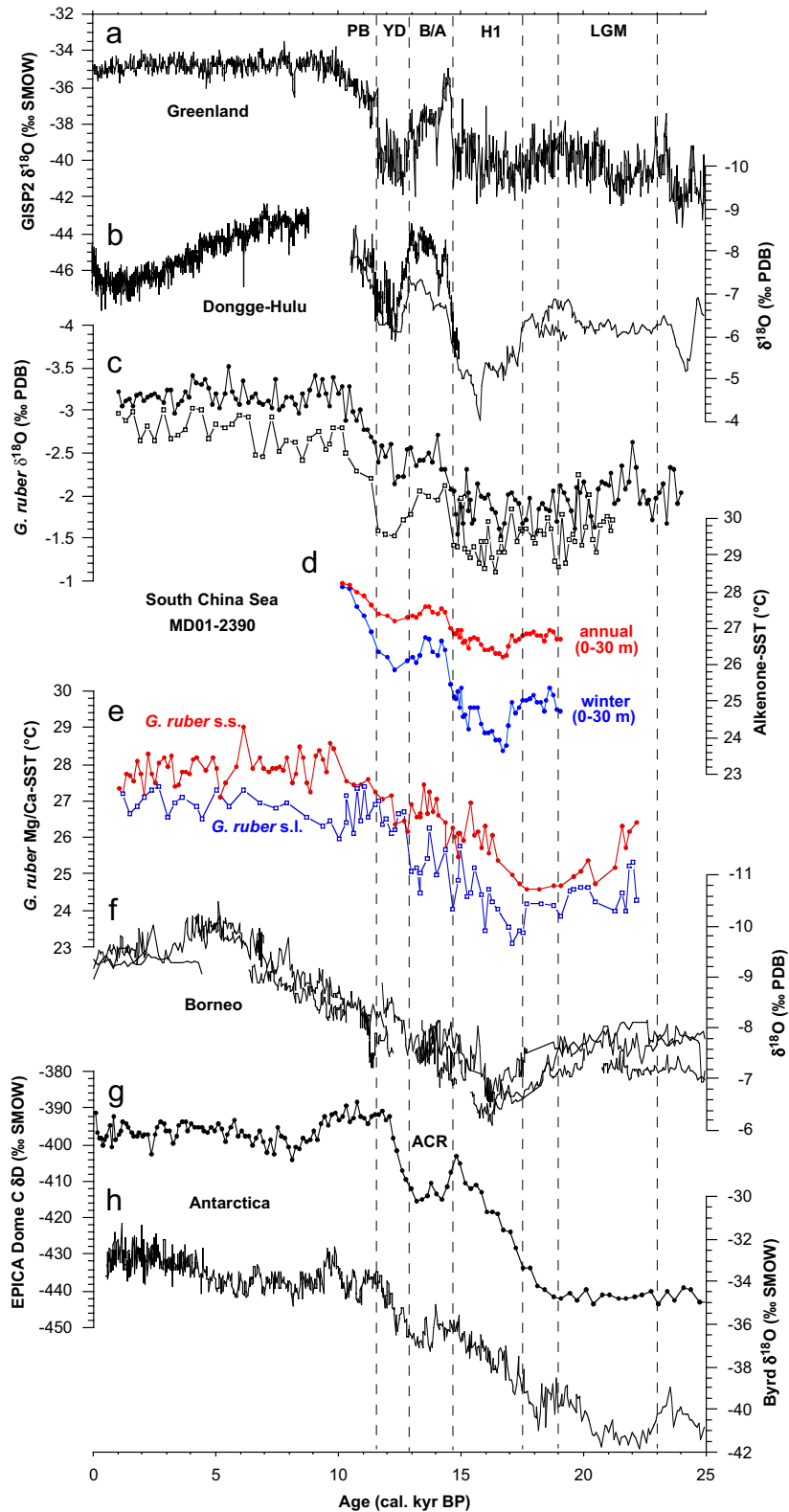


Fig. 4. Comparison of various climate records spanning the last deglaciation from the tropical southern SCS, eastern continental China, Borneo, Greenland and Antarctica. (a) $\delta^{18}\text{O}$ record from GISP2 (Stuiver and Grootes, 2000); (b) Stalagmite $\delta^{18}\text{O}$ record of EAM intensity from Dongge-Hulu Cave (Wang et al., 2001, 2005); (c) $\delta^{18}\text{O}$ records of *G. ruber sensu stricto* (s.s.; solid dots) and *G. ruber sensu lato* (s.l.; open squares) from the southern SCS (MD01-2390; this study); (d) Alkenone SST data of core MD01-2390, red: annual average SST estimates and blue: winter SST estimates (this study; see text for discussion); (e) Mg/Ca SST data on *G. ruber sensu stricto* (s.s.; red) and *G. ruber sensu lato* (s.l.; blue) of core MD01-2390 (this study); (f) Stalagmite $\delta^{18}\text{O}$ records from northern Borneo (Partin et al., 2007); (g) δD from EPICA Dome C (EPICA community members, 2004); and (h) $\delta^{18}\text{O}$ record from Byrd (Blunier et al., 1998). PB = Preboreal; YD = Younger Dryas; B/A = Bölling-Allerød; H1 = Heinrich event 1; LGM = Last Glacial Maximum; ACR = Antarctic Cold Reversal.

s.l.) show generally higher SST estimates for *G. ruber* s.s. when compared with *G. ruber* s.l. (Figs. 2 and 4). The mean temperature difference (ΔT) between *G. ruber* s.s. and *G. ruber* s.l. is 1.1 °C, which is close to the standard error of estimates (~ 1 °C) for various temperature calibrations derived from core tops and sediment trap calibrations (Elderfield and Ganssen, 2000; Lea et al., 2000; Dekens et al., 2002; Anand et al., 2003; Fig. 5a). However, the ΔT of many samples far exceeds the standard error of SST estimates for various Mg/Ca-temperature calibrations, indicating that the difference between the morphotype-specific SST estimates is not due to analytical uncertainties. A Student's *t*-test was performed in order to test if the difference in Mg/Ca-SST estimates between the two different morphotypes is significant. The Student's *t*-test yielded a *t*-value of 12.5, which exceeds the critical *t*-value of 2.0 for 60 degrees of freedom ($p = 0.05$). This indicates that the Mg/Ca-SST estimates of *G. ruber* s.s. and *G. ruber* s.l. are statistically significantly different. These findings together with previous isotopic studies from the SCS

(Wang, 2000; Löwemark et al., 2005) and from the subtropical gyre in the North Pacific (Kawahata, 2005) are suggested to reflect a different depth habitat of both morphotypes, with *G. ruber* s.s. inhabiting the upper ~ 30 m of the water column and *G. ruber* s.l. inhabiting depths below ~ 30 m. This scenario is supported by plankton tow and pumping samples, which suggest that *G. ruber* s.s. is predominant in the surface waters while *G. ruber* s.l. is predominant in deeper waters in the seas around Japan (Kuroyanagi and Kawahata, 2004).

The *G. ruber* s.s. derived Mg/Ca SST record reveals a continuous deglacial warming without any intermittent cooling during H1. The sign and the relative timing (within the present age model and sample resolution) of the early deglacial *G. ruber* s.s. Mg/Ca-based warming resemble features of the warming patterns observed in Mg/Ca-SST records from the Sulu Sea (Rosenthal et al., 2003), the Makassar Strait (Visser et al., 2003), and the western and eastern open Pacific (Lea et al., 2000, 2006; Fig. 1). In contrast to these records, however, the *G. ruber* s.s.-derived

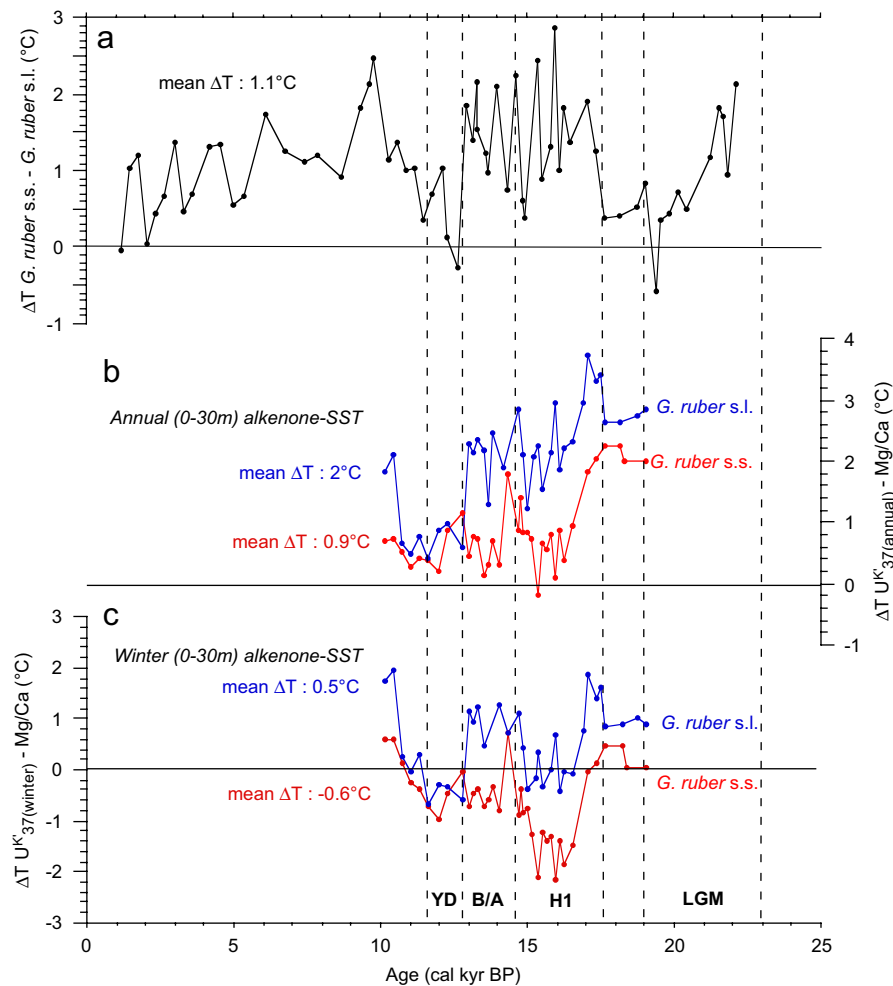


Fig. 5. (a) Temperature difference (ΔT) between *G. ruber* sensu stricto (s.s.) and *G. ruber* sensu lato (s.l.). Note that for many samples ΔT far exceeds the standard error of Mg/Ca-SST estimates (see text for discussion). (b) Temperature difference between the alkenone annual mean SST estimates and Mg/Ca SST estimates of the two *G. ruber* morphotypes (red: *G. ruber* s.s.; blue: *G. ruber* s.l.); (c) Temperature difference between alkenone winter mean SST estimates and Mg/Ca SST estimates of the two *G. ruber* morphotypes (red: *G. ruber* s.s.; blue: *G. ruber* s.l.). Note the smaller ΔT between winter-time alkenone and Mg/Ca SST estimates compared to the ΔT between annual average alkenone and Mg/Ca estimates (see text for discussion).

record suggests a subtle decrease in temperature during the YD, similar to the alkenone SST record. In contrast to the *G. ruber* s.s. record, *G. ruber* s.l. Mg/Ca SST estimates suggest a cooling synchronous with the “H1 event” in the alkenone record, but show no cooling during the YD. Although highly speculative, it appears that these discrepancies may reflect temporal changes in the preferred habitat or seasonality of the two *G. ruber* morphotypes. The southern SCS Mg/Ca records thus appear to show a link to southern as well as northern hemisphere deglaciation, whereas the alkenone unsaturation-based SST estimates reveal a “Greenland-type warming” (sensu Kienast and Kienast, 2005). In summary, the SST records examined here suggest a diverse pattern of proxy carrier-dependent temporal changes of the tropical SCS during the last deglaciation.

In contrast to the Mg/Ca-SST records, both morphotype-specific *G. ruber* stable oxygen isotope records closely follow the alkenone-based SST records (Fig. 4). Previous alkenone records from the tropical SCS show a similar parallelism between alkenone and *G. ruber* $\delta^{18}\text{O}$ (Kienast et al., 2001). A “lead” of Mg/Ca-SST vs planktonic foraminiferal $\delta^{18}\text{O}$ (and $\delta^{18}\text{O}_{\text{sw}}$) is consistent with studies from the Sulu Sea (Rosenthal et al., 2003), the Makassar Strait (Visser et al., 2003), and the western Pacific (Lea et al., 2000). We propose that the apparent divergence of *G. ruber* $\delta^{18}\text{O}$ and Mg/Ca during the time interval 17.5–15 ka BP (H1) is most likely related to the fact that the temperature effect on the $\delta^{18}\text{O}_{\text{calcite}}$ signal is suppressed by a strong $\delta^{18}\text{O}_{\text{seawater}}$ effect associated with a change in the ratio of the amount of summer precipitation to winter precipitation on the *G. ruber* $\delta^{18}\text{O}$ record during the time interval of H1. This interpretation is consistent with the decreased strength of the summer East Asian monsoon (EAM) and associated change in the ratio of the amount of summer precipitation to winter precipitation as inferred from the $\delta^{18}\text{O}$ of Borneo (Partin et al., 2007) and Hulu Cave stalagmites (Wang et al., 2001; Fig. 4). This interpretation is also supported by model simulations (Zhang and Delworth, 2005; Jin et al., 2007) that predict a weakening of summer monsoon intensity associated with a decrease in summer monsoon precipitation in south and southeast Asia during Heinrich events. Thus, a substantial decrease in precipitation and change in the ratio of the amount of summer and winter precipitation may have led to heavier planktonic foraminiferal $\delta^{18}\text{O}$. This is due to a higher proportion of winter rainfall with heavier $\delta^{18}\text{O}$ values than the summer rainfall (Wang et al., 2001; Oppo et al., 2003) in the southern SCS during the time interval of H1, suppressing the SST component on the $\delta^{18}\text{O}_{\text{calcite}}$ values. This interpretation is in good agreement with the concept of Dannenmann et al. (2003) and Rosenthal et al. (2003), who showed that millennial-scale variability in hydrography in this region is primarily driven by changes in sea surface salinity (SSS). The strong link to the summer EAM development and by inference to millennial-scale climate variability over Greenland supports the notion of

an atmospheric coupling with changes in the high northern latitudes (e.g. Wang et al., 2001; Rosenthal et al., 2003). The overriding control of the (local/regional) hydrography on the planktonic foraminiferal $\delta^{18}\text{O}$ thus cautions the interpretation of tropical planktonic foraminiferal $\delta^{18}\text{O}$ as direct recorder of changes in continental ice volume.

3.2. Causes for the proxy dependence of the temporal pattern of deglacial warming

In his commentary, Mix (2006) proposed three mechanisms that could account for the discrepancy of U_{37}^{K} and Mg/Ca in recording deglacial warming in the EEP: (a) physiological effects on U_{37}^{K} ; (b) oceanographic/preservation effects on Mg/Ca and/or alkenones; and (c) different seasonal preferences of coccolithophorids and planktonic foraminifera. We will explore all three possibilities in light of our new records from the SCS.

(a) Culture experiments by Prahl et al. (2006) have shown that coccolithophores grown under nutrient limitation tend to record colder temperatures. Thus, alkenone-based SST reconstructions of a cooling during the H1 time interval could potentially be caused by decreased nutrient availability, resulting in colder temperature estimates. This interpretation might be supported by model simulations that predict a global reduction in productivity due to a decrease in upwelling and associated depletion of upper ocean nutrients in response to a reduction in the Atlantic overturning circulation (Schmittner, 2005). Higher primary productivity as deduced from higher organic carbon fluxes and accumulation, however, has been reported from the southern SCS during the last glacial (e.g. Jian et al., 1999; Kuhnt et al., 1999; Jia and Peng, 2002; Wei et al., 2003). Notably, none of these records shows any significant decrease in productivity during H1. It is further suggested that nutrient input from rivers of the vast exposed shelves could have enhanced the nutrient availability in the glacial SCS surface waters, most likely resulting in higher primary productivity (Jia et al., 2006). Higher glacial primary productivity between ~25 and ~14.9 ka BP has also been deduced from lower abundances of the coccolithophore *Florisphaera profunda* (core 17961, Fig. 1; Pelejero et al., 1999b). From the available data, it thus appears that nutrient limitation is not a viable candidate for explaining the cooling signal recorded by alkenones in the southern SCS during the time interval of H1. Like in the SCS, it is unlikely that nutrient stress affected the alkenone SST estimates in the EEP. There, the H1 cooling is associated with maximal primary productivity as inferred from C_{org} percentage and ^{230}Th normalized fluxes (Kienast et al., 2006; see below). Furthermore, the alkenone records from the SCS and EEP display the same cooling associated with H1 (Kienast et al. 2006), even though the SCS and EEP are characterized by fundamentally different physico-environmental conditions and biogeochemical dynamics over the last deglaciation. This suggests that nutrient depletion (physiological effects) on the U_{37}^{K} SST estimates is not the

primary cause for the disagreement between alkenones and Mg/Ca ratios.

(b) Similar to the southern SCS SST records, the contrasting pattern of deglacial warming is observed from alkenone (Kienast et al., 2006; Prah et al., 2006) and Mg/Ca records (Lea et al., 2000, 2006) in the EEP, suggesting a pan-tropical Pacific phenomenon (see also above). A number of effects have been proposed to affect SST estimates as recorded by foraminiferal Mg/Ca or alkenones, such as local changes in salinity (Nürnberg et al., 1996; Lea et al., 1999), pH (Lea et al., 1999; Russell et al., 2004), carbonate ion concentration (Russell et al., 2004) and post-depositional dissolution (e.g. Brown and Elderfield, 1996; Rosenthal et al., 2000; Regenberg et al., 2006) for Mg/Ca, or lateral advection (Ohkouchi et al. 2002; Mollenhauer et al. 2005) and differential degradation (Hoefs et al., 1998; Gong and Hollander, 1999) for alkenones. Although the influence of salinity, pH and carbonate ion as determined by culture experiments are expected to have a minor influence on the incorporation of shell Mg, the combined effect of these factors could conceivably exert a significant influence on the Mg/Ca-based palaeotemperature estimates. For example, assuming a deglacial increase in salinity of 1 psu between 19 to 15 ka BP (Rosenthal et al., 2003 in the Sulu Sea; core MD97-2141), a decrease in pH by ~ 0.2 pH units (estimated for the western Pacific by Palmer and Pearson, 2003; ERDC-92, Fig. 1) and a decrease in seawater carbonate ion concentration of ~ 20 $\mu\text{mol/kg}$ (in analogy to estimates by Barker and Elderfield, 2002 from the North Atlantic), the combined salinity, pH and seawater carbonate ion influence would be equivalent to a positive temperature bias of ~ 1.5 $^{\circ}\text{C}$ (assuming a 10% increase in Mg/Ca per $^{\circ}\text{C}$), when using the experimentally determined responses on the Mg/Ca for *G. bulloides* (Lea et al., 1999; Russell et al., 2004). However, it is unreasonable to assume a homogenous and pan-tropical Pacific change in all these parameters of this magnitude, thus rendering secondary effects on Mg/Ca to explain the early warming very unlikely. Similarly, the observation of a U_{37}^{K} cold event during the time interval of H1 at sites with very different sedimentation regimes, rates and organic carbon contents suggests that differential preservation or lateral advection are unlikely candidates to explain the cold U_{37}^{K} SST estimates.

Finally, preservational effects on foraminiferal Mg/Ca have also been considered by Mix (2006) to explain the apparent discrepancy between the alkenone and Mg/Ca SST estimates. The last deglaciation is regarded as a time of enhanced calcite preservation as inferred from planktonic foraminiferal shell weights in the Pacific (e.g. Marchitto et al., 2005) and in the Caribbean Sea (Broecker et al., 2003). A better calcite preservation could have led to higher Mg/Ca ratios and, thus, a warm bias of the Mg/Ca temperatures during the last deglaciation. However, the planktonic foraminiferal fragmentation index and the occurrence of pteropods throughout core MD01-2390

indicate excellent calcite preservation during the entire record (Steinke et al., 2006), and no prominent preservation peak centered between 20 to 15 ka BP is observed. Although no paired qualitative proxy records for carbonate preservation and Mg/Ca SST estimates are available from other sites, given the observation of an early warming in Mg/Ca SST estimates throughout the tropical Pacific independent of core depth, it is most unlikely that the Mg/Ca SST estimates are biased by calcite preservational effects (see also Lea et al., 2006).

(c) The most likely and parsimonious explanation for the discrepancy between Mg/Ca- and U_{37}^{K} -based estimates of the deglacial warming in the SCS (and elsewhere) are differences in the seasonal preference (optimum habitat conditions) of planktonic foraminifera *G. ruber* and alkenone-producing coccolithophores. We thus speculate that alkenones primarily record changes in winter EAM, which is closely coupled to the climate history of the North Atlantic region, whereas *G. ruber* mostly record an annual average SST and $\delta^{18}\text{O}$ signal, possibly weighted toward the summer months. A literature survey shows that the alkenone-producing *Gephyrocapsa oceanica* tends to dominate in highly fertile waters in a well mixed/turbulent upper water column whereas *Emiliania huxleyi* display a broader ecological tolerance (Okada and Honjo, 1973; Molino and McIntyre, 1990). A recent sediment trap study together with water sampling from the northern SCS showed that alkenone-producing coccolithophores (*E. huxleyi*; *G. oceanica*) are predominant in cold months (winter and spring) when the northeastern monsoon prevailed (Chen et al., 2007), suggesting that the winter EAM season with nutrient-rich upper surface waters represents favorable conditions for alkenone-producing coccolithophores. The latter finding is consistent with an earlier sediment trap study by Wiesner et al. (1996) from the northern SCS, which showed that coccolithophores are most abundant during the winter monsoon season. Although no data are currently available on the seasonality of coccolithophores in the southern SCS, chlorophyll levels are highest during the winter and spring season (Liu et al., 2002). This is indicative of highest productivity levels, and, by inference, highest coccolithophore abundances in the southern SCS during the winter and spring. In contrast, *G. ruber* has been shown to be most abundant in oligotrophic, stratified waters (Bé, 1982; Fairbanks et al., 1982). Sediment trap studies by Wiesner et al. (1996) and Lin et al. (2004) show that highest fluxes of *G. ruber* are weighted toward the warm months (August through October) with smaller contributions during the rest of the year. In contrast, Tian et al. (2005) found that *G. ruber* is more abundant during winter (from December to March). Inconsistencies between the different studies may be attributed to the different collection years that are potentially masked by interannual variations (ENSO imprints), the short collection periods (maximum 3 yr), and/or the different sampling sites. In addition, plankton tow studies from the western Pacific have shown that

G. ruber is preferentially abundant during the summer season (Troelstra and Kroon, 1989), which is consistent with sediment trap experiments in the western Pacific (Kawahata et al., 2002).

The interpretation of the discrepancy between Mg/Ca- and $U_{37}^{K'}$ -based SST estimates of the deglacial warming in the SCS as caused by seasonality, however, seems to be in conflict with the relative amplitude of the deglacial changes in temperature implied by the different records (Figs. 2 and 4) as well as with the relatively warmer $U_{37}^{K'}$ SST estimates compared to the Mg/Ca ratios between 19 and 10 ka BP (Fig. 5b). Thus, the alkenone record suggests an increase in temperature between H1 and 10 ka BP of about 2 °C, while the Mg/Ca-based records suggest a larger warming, on the order of 3 °C (Fig. 4). Due to an intensification of the glacial winter monsoon (Wang and Wang, 1990; Wang et al., 1995), one would expect that winter SST changes (enhanced LGM seasonality) are generally larger, and, according to the inferred seasonality, alkenones should thus record a larger cooling during the last glaciation compared with Mg/Ca ratios. We speculate that this apparent conflict is due to the fact that annual mean 0–30 m temperatures (Pelejero and Grimalt, 1997) were used for the $U_{37}^{K'}$ /SST calibration. Using a linear regression for cold season (winter) SSTs at 0–30 m instead ($U_{37}^{K'} = 0.014T + 0.573$; Pelejero and Grimalt, 1997), the season of maximal coccolithophorid growth/alkenone production, yields Late glacial temperatures around 24–25 °C, and, in turn, a warming of ~4 °C between H1 and 10 ka BP (Fig. 4). The ΔT values between winter-time alkenone and Mg/Ca SST estimates are smaller compared to the ΔT between annual average alkenone and Mg/Ca estimates (Fig. 5c). The alkenones show colder or only slightly warmer SST estimates compared to the morphotype-specific Mg/Ca SST estimates (Fig. 5c). These “winter-time” $U_{37}^{K'}$ estimates are consistent with the notion of an enhanced glacial seasonality due to an intensification of the glacial winter monsoon as suggested by Wang and Wang (1990) and Wang et al. (1995). Given the seasonal preference of alkenone-producing coccolithophores for the winter season (see discussion above), and the same high R values ($R = 0.93$) for SCS $U_{37}^{K'}$ vs winter and $U_{37}^{K'}$ vs annual temperatures (Pelejero and Grimalt, 1997), there is no a priori reason to apply the annual $U_{37}^{K'}$ /SST equation instead of the winter equation to estimate past SSTs.

Interpretation of the $U_{37}^{K'}$ SST estimates during the time interval of H1 as a reflection of cooling, primarily during the winter months, is also consistent with the hypothesis of Denton et al. (2005), that winter climate was the common linkage between Greenland-European temperatures and Asian monsoons during the last glaciation, particularly during Heinrich events. Thus, severe changes in winter climate (seasonality changes) in the northern hemisphere could have amplified and propagated a signal of abrupt change throughout the northern hemisphere and into the tropics (Denton et al., 2005). This could explain the coeval changes in southern SCS alkenone SSTs and the tempera-

ture history over Greenland/Europe. In contrast, SST changes recorded by foraminiferal Mg/Ca in the northern SCS and the tropical Pacific have been inferred to be driven by a complex interplay of summer EAM changes (e.g. Oppo and Sun, 2005), tropical dynamics (ENSO variability; Dannenmann et al., 2003; Rosenthal et al., 2003) and/or greenhouse gas forcing (Lea et al., 2006). The inference of a predominant winter-time cooling of the SCS during deglaciation is also supported by high relative abundances of *N. pachyderma* (dextral) in the southern SCS. These have been interpreted to reflect a considerable decrease in winter SSTs compared to modern conditions due to an intrusion of cold surface water from the northeast via the Bashi Strait as the combined result of an intensified winter monsoon, a southward shift of the polar front and an eastward migration of the Kuroshio Current (Wang and Wang, 1990; Miao et al., 1994; Wang et al., 1995).

Although the *G. ruber* $\delta^{18}O$ is also affected by winter monsoon precipitation, which has a heavier $\delta^{18}O$ signature, *G. ruber* predominantly records an annual average SST and $\delta^{18}O$ signal, possibly weighted toward the summer months. This is inferred from the close correspondence between the $\delta^{18}O$ records to the Hulu Cave stalagmites, and from sediment trap studies on the seasonal abundance of planktonic foraminifera in the SCS (see discussion above). By the same token, the close agreement between $\delta^{13}C$ and the difference between foraminiferal Mg/Ca vs $U_{37}^{K'}$ SST estimates in the EEP pointed out by Mix (2006) could be interpreted as SST signal during the upwelling season recorded by the alkenones, with a $\delta^{13}C$ signature that affects the water column and thus by inference the planktonic foraminiferal isotope signature, year-round.

In summary, our interpretation of the SCS SST estimates adds to the growing body of literature that invokes differences in seasonal habitat preferences of alkenone-producing coccolithophores and planktonic foraminifera to explain contrasting SST estimates between the two proxy carriers (de Vernal et al., 2006; Came et al., 2007). For example, Haug et al. (2005; North Pacific), Seki et al. (2004; Sea of Okhotsk), Ishiwatari et al. (1999; Japan Sea) and Chapman et al. (1996; subtropical North Atlantic) also interpreted $U_{37}^{K'}$ records to represent seasonal SST estimates. The *G. ruber* Mg/Ca SST estimates revealing morphotype-specific and opposing responses to the YD and H1 events could point toward changes in seasonal habitat preferences through time. Similarly, Chapman et al. (1996) and Seki et al. (2004) proposed discrepancies between different proxy records and/or anomalous SST estimates to reflect a shift in the season of maximum coccolithophorid production.

4. Summary and conclusions

Deglacial warming of the SCS, as recorded by alkenones is punctuated by a decrease in temperature during the time

interval of H1, while the morphotype-specific *G. ruber* Mg/Ca SST estimates suggest a complex pattern of temporal changes of the tropical SCS during the last deglaciation: *G. ruber* s.s. Mg/Ca SST estimates suggest a continuous warming starting around 18 ka BP without any marked response to H1, whereas *G. ruber* s.l. Mg/Ca SST estimates reveal a cooling around ~17–15 ka BP that is similar to the cooling observed in the alkenone SST record. This proxy-dependent difference in recording the deglacial warming is similar to other records from the tropical Pacific. We propose that this discrepancy is due to differences in seasonality of *G. ruber* morphotypes and alkenone-producing coccolithophores. We speculate that alkenones primarily record changes in the winter East Asian monsoon, which is coupled to the climate history of the North Atlantic region, whereas *G. ruber* morphotypes record mostly an annual average SST and $\delta^{18}\text{O}$ signal, possibly weighted toward the summer months, sharing imprints of northern and southern hemisphere climate change and/or tropical dynamics (e.g. ENSO). Due to the discrepancies of the morphotype-specific *G. ruber* records in recording the last deglaciation, it appears that these differences reflect temporal changes in the preferred seasonality or depth habitat of the two *G. ruber* morphotypes. In contrast to the Mg/Ca-SST records, both morphotype-specific *G. ruber* stable oxygen isotope records closely follow the alkenone-based SST records with a clear $\delta^{18}\text{O}$ maximum during the H1 time interval. The apparent divergence of *G. ruber* $\delta^{18}\text{O}$ and Mg/Ca during this time interval is most likely related to the fact that the temperature effect on the $\delta^{18}\text{O}_{G. ruber}$ signal is suppressed by a strong $\delta^{18}\text{O}_{\text{seawater}}$ effect on the *G. ruber* $\delta^{18}\text{O}$ record during the time interval of H1, which is associated with a change in the ratio of the amount of summer to winter precipitation. This interpretation is consistent with proxy evidence and model simulations of a weakened summer monsoon intensity associated with a decrease in summer monsoon precipitation in south and southeast Asia during the time interval H1.

Acknowledgments

We thank the IMAGES Program for allowing access to core MD01-2390. This study has been funded by the Deutsche Forschungsgemeinschaft (DFG) through the Research Center Ocean Margins (RCOM), University of Bremen, and by the National Science Council (NSC), Taiwan, through grants to MTC (NSC91-2611-M-019-012-IM, NSC91-2811-M-019-002). MK acknowledges funding from Natural Science and Engineering Research Council of Canada (NSERC) and the Canadian Institute for Advanced Research (CIFAR). JG thanks RCOM for financial support via an RCOM fellowship. We express our gratitude to M. Segl and her team for stable isotope analyses. We thank I. Meyer and A. Nagel for technical assistance. Thanks go to D. Oppo and D. Lea for thoughtful comments on this study. The data in this study

are archived and can be retrieved at PANGAEA (Publishing Network for Geoscientific and Environmental Data). RCOM contribution 0548.

References

- Anand, P., Elderfield, H., Conte, M.H., 2003. Calibration of Mg/Ca thermometry in planktonic foraminifera from a sediment trap time series. *Paleoceanography* 18, doi:10.1029/2002PA000846.
- Barker, S., Elderfield, H., 2002. Foraminiferal calcification response to glacial–interglacial changes in atmospheric CO₂. *Science* 297, 833–836.
- Barker, S., Greaves, M., Elderfield, H., 2003. A study of cleaning procedures used for foraminiferal Mg/Ca paleothermometry. *Geochemistry, Geophysics, Geosystems* 4, doi:10.1029/2003GC000559.
- Bé, A.W.H., 1982. Biology of planktonic foraminifera. In: Broadhead, T.W. (Ed.), *Foraminifera: Notes For a Short Course. Studies in Geology*, vol. 6. University of Tennessee, pp. 51–92.
- Blunier, T., Chapellaz, J., Schwander, J., Dällenbach, A., Stauffer, B., Stocker, T.F., Raynaud, D., Jouzel, J., Clausen, H.B., Hammer, C.U., Johnsen, S.J., 1998. Asynchrony of Antarctic and Greenland climate change during the last glacial period. *Nature* 394, 739–743.
- Broecker, W.S., Clark, E., Droxler, A.W., 2003. Shell weights from intermediate depths in the Caribbean Sea. *Geochemistry, Geophysics, Geosystems* 4, doi:10.1029/2002GC000491.
- Brown, S.J., Elderfield, H., 1996. Variations in Mg/Ca and Sr/Ca ratios of planktonic foraminifera caused by postdepositional dissolution: evidence of shallow Mg-dependent dissolution. *Paleoceanography* 11, 543–551.
- Came, R.E., Oppo, D.W., McManus, J.F., 2007. Amplitude and timing of temperature and salinity variability in the subpolar North Atlantic over the past 10 k.y. *Geology* 35, 315–318.
- Cane, M.A., 1998. A role for the tropical Pacific. *Science* 282, 59–61.
- Cayre, O., Bard, E., 1999. Planktonic foraminiferal and alkenone records of the last deglaciation from the eastern Arabian Sea. *Quaternary Research* 52, 337–342.
- Chapman, M.R., Shackleton, N.J., Zhao, M., Eglinton, G., 1996. Faunal and alkenone reconstructions of subtropical North Atlantic surface hydrography and paleotemperature over the last 28 kyr. *Paleoceanography* 11, 343–357.
- Chen, M.-T., Huang, C.-C., Pflaumann, U., Waelbroeck, C., Kucera, M., 2005. Estimating glacial western Pacific sea-surface temperature: methodological overview and data compilation of surface sediment planktic foraminifer faunas. *Quaternary Science Reviews* 24, 1049–1062.
- Chen, Y.-I.L., Chen, H.-Y., Chung, C.-W., 2007. Seasonal variability of coccolithophore abundance and assemblage in the northern South China Sea. *Deep-Sea Research II* 54, 1617–1633.
- Clement, A.C., Seager, R., Cane, M.A., 1999. Orbital controls on the El Niño/Southern Oscillation and the tropical climate. *Palaeoceanography* 14, 441–456.
- Conte, M.H., Sicre, M.-A., Rühlemann, C., Weber, J.C., Schulte, S., Schulz-Bull, D., Blanz, T., 2006. Global temperature calibration of the alkenone unsaturation index (U_{37}^K) in surface waters and comparison with surface sediments. *Geochemistry, Geophysics, Geosystems* 7, doi:10.1029/2005GC001054.
- Dannenmann, S., Linsley, B.K., Oppo, D.W., Rosenthal, Y., Beaufort, L., 2003. East Asian monsoon forcing of suborbital variability in the Sulu Sea during Marine Isotope Stage 3: link to northern hemisphere climate. *Geochemistry, Geophysics, Geosystems* 4, doi:10.1029/2002GC000390.
- de Garidel-Thoron, D.T., Rosenthal, Y., Beaufort, L., Bard, E., Sonzogni, C., Mix, A.C., 2007. A multiproxy assessment of the western equatorial Pacific hydrography during the last 30 kyr. *Paleoceanography* 22, doi:10.1029/2006PA001269.
- De Vernal, A., Rosell-Melé, A., Kucera, M., Hillaire-Marcel, C., Eynaud, F., Weinelt, M., Dokken, T., Kageyama, M., 2006. Comparing proxies for the reconstruction of LGM sea-surface conditions in the northern North Atlantic. *Quaternary Science Reviews* 25, 2820–2834.

- Dekens, P.S., Lea, D.W., Pak, D.K., Spero, H.J., 2002. Core top calibration of Mg/Ca in tropical foraminifera: refining paleotemperature estimation. *Geochemistry, Geophysics, Geosystems* 3, doi:10.1029/2001GC000200.
- Denton, G.H., Alley, R.B., Comer, G.C., Broecker, W.S., 2005. The role of seasonality in abrupt climate change. *Quaternary Science Reviews* 24, 1159–1182.
- Elderfield, H., Ganssen, G., 2000. Past temperature and $\delta^{18}\text{O}$ of surface ocean waters inferred from foraminiferal Mg/Ca ratios. *Nature* 405, 442–445.
- EPICA community members, 2004. Eight glacial cycles from an Antarctic ice core. *Nature* 429, 623–628.
- Fairbanks, R.G., Sverdrlove, M., Free, R., Wiebe, P.H., Bé, A.W.H., 1982. Vertical distribution and isotopic fractionation of living planktonic foraminifera from the Panama Basin. *Nature* 298, 841–844.
- Gong, C., Hollander, D.J., 1999. Evidence for the differential degradation of alkenone under contrasting bottom water oxygen conditions: implication for paleotemperature reconstructions. *Geochimica et Cosmochimica Acta* 63, 405–411.
- Haug, G.H., Ganopolski, A., Sigman, D.M., Rosell-Melé, A., Swann, G.E.A., Tiedemann, R., Jaccard, S.L., Bollmann, J., Maslin, M.A., Leng, M.J., Eglinton, G., 2005. North Pacific seasonality and the glaciation of North America 2.7 million years ago. *Nature* 433, 821–825.
- Hoefs, M.J.L., Versteegh, G.J.M., Rijpstra, W.I.C., Leeuw, J.W., Sinninghe Damste, J.S., 1998. Postdepositional oxic degradation of alkenones: implication for the measurement of palaeo sea surface temperature. *Paleoceanography* 13, 42–49.
- Hostetler, S., Piasias, N., Mix, A., 2006. Sensitivity of Last Glacial Maximum climate to uncertainties in tropical and subtropical ocean temperatures. *Quaternary Science Reviews* 25, 1168–1185.
- Ishiwatari, R., Yamada, K., Matsumoto, K., Houtatsu, M., Naraoka, H., 1999. Organic molecular and carbon isotopic records of the Japan Sea over the past 30 kyr. *Paleoceanography* 14, 260–270.
- Jia, G., Peng, P., 2002. Burial of different types of organic carbon in core 17962 from South China Sea since the last glacial period. *Quaternary Research* 58, 93–100.
- Jia, G., Xie, H., Peng, P., 2006. Contrast in surface water $\delta^{18}\text{O}$ distribution between the last Glacial Maximum and Holocene in the southern South China Sea. *Quaternary Science Reviews* 25, 1053–1064.
- Jian, Z., Wang, L., Kienast, M., Sarnthein, M., Kuhnt, W., Lin, H., Wang, P., 1999. Benthic foraminiferal paleoceanography of the South China Sea over the last 40,000 years. *Marine Geology* 156, 159–186.
- Jin, L., Chen, F., Ganopolski, A., Claussen, M., 2007. Response of East Asian climate to Dansgaard/Oeschger and Heinrich events in a coupled model of intermediate complexity. *Journal of Geophysical Research* 112, doi:10.1029/2006JD007316.
- Kawahata, H., 2005. Stable isotopic composition of two morphotypes of *Globigerinoides ruber* (white) in the subtropical gyre in the North Pacific. *Paleontological Research* 9, 27–35.
- Kawahata, H., Nishimura, A., Gagan, M.K., 2002. Seasonal change in foraminiferal production in the western equatorial Pacific warm pool: evidence from sediment trap experiments. *Deep-Sea Research II* 49, 2783–2800.
- Kiefer, T., Kienast, M., 2005. Patterns of deglacial warming in the Pacific Ocean: a review with emphasis on the time interval of Heinrich event 1. *Quaternary Science Reviews* 24, 1063–1081.
- Kienast, M., Steinke, S., Statterger, K., Calvert, S.E., 2001. Synchronous tropical South China Sea SST change and Greenland warming during deglaciation. *Science* 291, 2132–2134.
- Kienast, M., Kienast, S.S., Calvert, S.E., Eglinton, T.I., Mollenhauer, G., Francois, R., Mix, A.C., 2006. Eastern Pacific cooling and Atlantic overturning circulation during the last deglaciation. *Nature* 443, 846–849.
- Kuhnt, W., Hess, S., Jian, Z., 1999. Quantitative composition of benthic foraminiferal assemblages as a proxy indicator for organic carbon flux rates in the South China Sea. *Marine Geology* 156, 123–157.
- Kuroyanagi, A., Kawahata, H., 2004. Vertical distribution of living planktonic foraminifera in the seas around Japan. *Marine Micro-paleontology* 53, 173–196.
- Lea, D.W., 2003. Elemental and isotopic proxies of past ocean temperatures. In: Elderfield, H. (Ed.), *The Oceans and Marine Geochemistry*. Elsevier-Pergamon, Oxford, pp. 365–390.
- Lea, D.W., Mashiotta, T.A., Spero, H.J., 1999. Controls on magnesium and strontium uptake in planktonic foraminifera determined by live culturing. *Geochimica et Cosmochimica Acta* 63, 2369–2379.
- Lea, D.W., Pak, D.K., Spero, H.J., 2000. Climate impact of late Quaternary equatorial Pacific sea surface temperature variations. *Science* 289, 1719–1724.
- Lea, D.W., Pak, D.K., Belanger, C.L., Spero, H.J., Hall, M.A., Shackleton, N.J., 2006. Paleoclimate history of Galapagos surface waters over the last 135,000 yr. *Quaternary Science Reviews* 25, 1152–1167.
- Lin, H.-L., Wang, W.-C., Hung, G.-W., 2004. Seasonal variation of planktonic foraminiferal isotopic composition from sediment traps in the South China Sea. *Marine Micropaleontology* 53, 447–460.
- Liu, K.-K., Chao, S.-Y., Shaw, P.-T., Gong, G.-C., Chen, C.-C., Tang, T.-Y., 2002. Monsoon-forced chlorophyll distribution and primary production in the South China Sea: observations and a numerical study. *Deep-Sea Research I* 49, 1387–1412.
- Löwemark, L., Hong, W.L., Yui, T.-F., Hung, G.-W., 2005. A test of different factors influencing the isotopic signal of planktonic foraminifera in surface sediments from the northern South China Sea. *Marine Micropaleontology* 55, 49–62.
- Marchitto, T.M., Lynch-Stieglitz, J., Hemming, S.R., 2005. Deep Pacific CaCO_3 compensation and glacial–interglacial atmospheric CO_2 . *Earth and Planetary Science Letters* 231, 317–336.
- Miao, Q., Thunell, R.C., Anderson, D.M., 1994. Glacial–Holocene carbonate dissolution and sea surface temperatures in the South China and Sulu Seas. *Paleoceanography* 9, 269–290.
- Mix, A.C., 2006. Running hot and cold in the eastern equatorial Pacific. *Quaternary Science Reviews* 25, 1147–1149.
- Molfino, B., McIntyre, A., 1990. Processional forcing of nutricline dynamics in the equatorial Atlantic. *Science* 249, 766–769.
- Mollenhauer, G., Kienast, M., Lamy, F., Meggers, H., Schneider, R.R., Hayes, J.M., Eglinton, T.I., 2005. An evaluation of ^{14}C age relationship between co-occurring foraminifera, alkenones, and total organic carbon in continental margin sediments. *Paleoceanography* 20, doi:10.1029/2004PA001103.
- Nürnberg, D., Bijma, J., Hemleben, C., 1996. Assessing the reliability of magnesium in foraminiferal calcite as a proxy for water mass temperature. *Geochimica et Cosmochimica Acta* 60, 803–814.
- Nürnberg, D., Müller, A., Schneider, R.R., 2000. Paleo-sea surface temperature calculations in the equatorial east Atlantic from Mg/Ca ratios in planktonic foraminifera: a comparison to sea surface temperature estimates from U^{K}_{37} , oxygen isotopes, and foraminiferal transfer function. *Paleoceanography* 15, 124–134.
- Ohkouchi, N., Eglinton, T.I., Keigwin, L.D., Hayes, J.M., 2002. Spatial and temporal offsets between proxy records in a sediment drift. *Science* 298, 1224–1227.
- Okada, H., Honjo, S., 1973. The distribution of oceanic coccolithophorids in the Pacific. *Deep-Sea Research* 20, 355–374.
- Oppo, D.W., Sun, Y., 2005. Amplitude and timing of sea-surface temperature change in the northern South China Sea: dynamic link to the East Asian monsoon. *Geology* 33, 785–788.
- Oppo, D.W., Linsley, B.K., Rosenthal, Y., Dannemann, S., Beaufort, L., 2003. Orbital and suborbital climate variability in the Sulu Sea, western tropical Pacific. *Geochemistry, Geophysics, Geosystems* 4, doi:10.1029/2001GC000260.
- Pahnke, K., Sachs, J., Keigwin, L.D., Timmermann, A., Xie, S., 2007. Eastern tropical Pacific hydrologic changes during the past 27,000 years from D/H ratios in alkenones. *Paleoceanography*, doi:10.1029/2007PA001468.

- Partin, J.W., Cobb, K.M., Adkins, J.F., Clark, B., Fernandez, D.P., 2007. Millennial-scale trends in west Pacific warm pool hydrology since the Last Glacial Maximum. *Nature* 449, 452–456.
- Palmer, M.R., Pearson, P.N., 2003. A 23,000-year record of surface water pH and PCO₂ in the western equatorial Pacific Ocean. *Science* 300, 480–482.
- Pelejero, C., Grimalt, J.O., 1997. The correlation between the U₃₇^k index and sea surface temperatures in the warm boundary: the South China Sea. *Geochimica et Cosmochimica Acta* 61, 4789–4797.
- Pelejero, C., Grimalt, J.O., Heilig, S., Kienast, M., Wang, L., 1999a. High-resolution U₃₇^k temperature reconstructions in the South China Sea over the past 220 kyr. *Paleoceanography* 14, 224–231.
- Pelejero, C., Grimalt, J.O., Sarnthein, M., Wang, L., Flores, J.A., 1999b. Molecular biomarker record of sea surface temperature and climatic change in the South China Sea during the last 140,000 years. *Marine Geology* 156, 109–121.
- Pena, L.D., Calvo, E., Cacho, I., Eggins, S., Pelejero, C., 2005. Identification and removal of Mn–Mg-rich contaminant phases on foraminiferal tests: implications for Mg/Ca past temperature reconstructions. *Geochemistry, Geophysics, Geosystems* 6, doi:10.1029/2005GC000930.
- Prahl, F.G., Mix, A.C., Sparrow, M.A., 2006. Alkenone paleothermometry: biological lessons from marine sediment records off western South America. *Geochimica et Cosmochimica Acta* 70, 101–117.
- Regenberg, M., Nürnberg, D., Steph, S., Groeneveld, J., Garbeschönberg, D., Tiedemann, R., Dullo, W., 2006. Assessing the effect of dissolution on planktonic foraminiferal Mg/Ca ratios: evidence from Caribbean core tops. *Geochemistry, Geophysics, Geosystems* 7, doi:10.1029/2005GC001019.
- Rodgers, K.B., Lohmann, G., Lorenz, S., Schneider, R., Henderson, G.M., 2003. A tropical mechanism for northern hemisphere deglaciation. *Geochemistry, Geophysics, Geosystems* 4, doi:10.1029/2003GC000508.
- Rosenthal, Y., Lohmann, G.P., Lohmann, K.C., Sherrell, R.M., 2000. Incorporation and preservation of Mg in *G. sacculifer*: implications for reconstructing sea surface temperatures and the oxygen isotopic composition of seawater. *Paleoceanography* 15, 135–145.
- Rosenthal, Y., Oppo, D.W., Linsley, B.K., 2003. The amplitude and phasing of climate change during the last deglaciation in the Sulu Sea, western equatorial Pacific. *Geophysical Research Letters* 30, doi:10.1029/2002GL016612.
- Rottman, M.L., 1979. Dissolution of planktonic foraminifera and pteropods in South China Sea sediments. *Journal of Foraminiferal Research* 9, 41–49.
- Russell, A.D., Hönisch, B., Spero, H.J., Lea, D.W., 2004. Effects of seawater carbonate ion concentration and temperature on shell U, Mg, and Sr in cultured planktonic foraminifera. *Geochimica et Cosmochimica Acta* 68, 4347–4361.
- Schlitzer, R., 2007. Ocean Data View, <<http://odv.awi.de>>.
- Schmittner, A., 2005. Decline of the marine ecosystem caused by a reduction in the Atlantic overturning circulation. *Nature* 434, 628–633.
- Seki, O., Kawamura, K., Ikehara, M., Nakatsuka, T., Oba, T., 2004. Variation of alkenone sea surface temperature in the Sea of Okhotsk over the last 85 kyrs. *Organic Geochemistry* 35, 347–354.
- Shen, C.-C., Chiu, H.-Y., Chiang, H.-W., Chu, M.-F., Wei, K.-Y., Steinke, S., Chen, M.-T., Lin, Y.-S., Lo, L., 2007. High precision measurements of Mg/Ca and Sr/Ca ratios in carbonates by cold plasma inductively coupled plasma quadrupole mass spectrometry. *Chemical Geology* 236, 339–349.
- Steinke, S., Kienast, M., Pflaumann, U., Weinelt, M., Stattegger, K., 2001. A high-resolution sea-surface temperature record from the tropical South China Sea (16,500–3000 yr B.P.). *Quaternary Research* 55, 352–362.
- Steinke, S., Chiu, H.-Y., Yu, P.-S., Shen, C.-C., Löwemark, L., Mii, H.-S., Chen, M.-T., 2005. Mg/Ca ratios of two *Globigerinoides ruber* (white) morphotypes: Implications for reconstructing past tropical/subtropical surface water conditions. *Geochemistry, Geophysics, Geosystems* 6, doi:10.1029/2005GC000926.
- Steinke, S., Chiu, H.-I., Yu, P.-S., Shen, C.-C., Erlenkeuser, H., Löwemark, L., Chen, M.-T., 2006. On the influence of sea level and monsoon climate on the southern South China Sea freshwater budget over the last 22,000 years. *Quaternary Science Reviews* 25, 1475–1488.
- Stott, L., Poulsen, C., Lund, S., Thunell, R., 2002. Super ENSO and global climate oscillations at millennial time scales. *Science* 297, 222–226.
- Stuiver, M., Grootes, P.M., 2000. GISP2 oxygen isotope ratios. *Quaternary Research* 53, 277–284.
- Tian, J., Wang, P., Chen, R., Cheng, X., 2005. Quaternary upper ocean thermal gradient variations in the South China Sea: implications for east Asian monsoon climate. *Paleoceanography* 20, doi:10.1029/2004PA001115.
- Troelstra, S.R., Kroon, D., 1989. Note on extant planktonic Foraminifera from the Banda Sea, Indonesia (Snellius-II Expedition, cruise G5). *Netherlands Journal of Sea Research* 24, 459–463.
- Visser, K., Thunell, R.C., Stott, L.D., 2003. Magnitude and timing of temperature change in the Indo-Pacific warm pool during deglaciation. *Nature* 421, 152–155.
- Wang, L., 2000. Isotopic signals in two morphotypes of *Globigerinoides ruber* (white) from the South China Sea: implications for monsoon climate change during the last glacial cycle. *Palaeography, Palaeoclimatology, Palaeoecology* 161, 381–394.
- Wang, L., Wang, P., 1990. Late Quaternary paleoceanography of the South China Sea: glacial–interglacial contrasts in an enclosed basin. *Paleoceanography* 5, 77–90.
- Wang, L., Sarnthein, M., Erlenkeuser, H., Grimalt, J., Grootes, P., Heilig, S., Ivanova, E., Kienast, M., Pelejero, C., Pflaumann, U., 1999. East Asian monsoon climate during the Late Pleistocene: high-resolution sediment records from the South China Sea. *Marine Geology* 156, 245–284.
- Wang, P., Wang, L., Bian, Y., Jian, Z., 1995. Late Quaternary paleoceanography of the South China Sea: surface circulation and carbonate cycles. *Marine Geology* 127, 145–165.
- Wang, Y., Cheng, H., Edwards, R.L., He, Y., Kong, X., An, Z., Wu, J., Kelly, M.J., Dykoski, C.A., Li, X., 2005. The Holocene Asian monsoon: links to solar changes and North Atlantic climate. *Science* 308, 854–857.
- Wang, Y.J., Cheng, H., Edwards, R.L., An, Z.S., Wu, J.Y., Shen, C.-C., Dorale, J.A., 2001. A high-resolution, absolute-dated late Pleistocene monsoon record from Hulu Cave, China. *Science* 294, 2345–2348.
- Wei, G., Ying, L., Li, X., Chen, M., Wei, W., 2003. High-resolution elemental records from the South China Sea and their paleoproductivity implications. *Paleoceanography* 18, doi:10.1029/2002PA000826.
- Wefer, G., Berger, W.H., Bijma, J., Fischer, G., 1999. Clues to ocean history: a brief overview of proxies. In: Fischer, G., Wefer, G. (Eds.), *Use of Proxies in Paleoceanography: examples from the South Atlantic*. Springer, Berlin, Heidelberg, pp. 1–68.
- Weldeab, S., Schneider, R.R., Kölling, M., 2006. Comparison of foraminiferal cleaning procedures for Mg/Ca paleothermometry on core material deposited under varying terrigenous-input and bottom water conditions. *Geochemistry, Geophysics, Geosystems* 7, doi:10.1029/2005GC000990.
- Wiesner, M.G., Zheng, L., Wong, H.K., Wang, Y., Chen, W., 1996. Fluxes of particulate matter in the South China Sea. In: Ittekkot, V., Schäfer, P., Honjo, S., Depetris, P.J. (Eds.), *Particle Flux in the Ocean*. SCOPE, Wiley, New York, pp. 293–312.
- Yin, J.H., Battisti, D.S., 2001. The importance of tropical sea surface temperature patterns in simulations of Last Glacial Maximum climate. *Journal of Climate* 14, 565–581.
- Zhang, R., Delworth, T.L., 2005. Simulated tropical response to a substantial weakening of the Atlantic thermohaline circulation. *Journal of Climate* 18, 1853–1860.
- Zhao, M., Huang, C.-Y., Wang, C.-C., Wei, G., 2006. A millennial-scale U₃₇^k sea-surface temperature record from the South China Sea (8°N) over the last 150 Myr: monsoon and sea-level influence. *Palaeography, Palaeoclimatology, Palaeoecology* 236, 39–55.